

UC Davis

UC Davis Previously Published Works

Title

Deletion Timing of Cic Alleles during Hematopoiesis Determines the Degree of Peripheral CD4+ T Cell Activation and Proliferation.

Permalink

<https://escholarship.org/uc/item/5d8156h0>

Journal

Immune network, 20(5)

ISSN

1598-2629

Authors

Park, Guk-Yeol

Lee, Gil-Woo

Kim, Soeun

et al.

Publication Date

2020-10-01

DOI

10.4110/in.2020.20.e43

Copyright Information

This work is made available under the terms of a Creative Commons Attribution-NonCommercial License, available at <https://creativecommons.org/licenses/by-nc/4.0/>

Peer reviewed

Brief Communication



Deletion Timing of *Cic* Alleles during Hematopoiesis Determines the Degree of Peripheral CD4⁺ T Cell Activation and Proliferation

Guk-Yeol Park ¹, Gil-Woo Lee^{2,3}, Soeun Kim ¹, Hyebeen Hong ¹,
Jong Seok Park ¹, Jae-Ho Cho ^{3,*}, Yoontae Lee ^{1,2,*}

¹Department of Life Sciences, Pohang University of Science and Technology (POSTECH), Pohang 37673, Korea

²Division of Integrative Bioscience and Biotechnology, Pohang University of Science and Technology (POSTECH), Pohang 37673, Korea

³Medical Research Center for Combinatorial Tumor Immunotherapy, Immunotherapy Innovation Center, Department of Microbiology and Immunology, Chonnam National University Medical School, Hwasun Hospital, Hwasun 58128, Korea

OPEN ACCESS

Received: Jul 31, 2020

Revised: Oct 5, 2020

Accepted: Oct 8, 2020

*Correspondence to

Jae-Ho Cho

Medical Research Center for Combinatorial Tumor Immunotherapy, Immunotherapy Innovation Center, Department of Microbiology and Immunology, Chonnam National University Medical School, Hwasun Hospital, 322 Seoyang-ro, Hwasun-eup, Hwasun 58128, Korea.
E-mail: jh_cho@chonnam.ac.kr

Yoontae Lee

Department of Life Sciences and Division of Integrative Bioscience and Biotechnology, Pohang University of Science and Technology (POSTECH), 7 Cheongam-ro, Nam-gu, Pohang 37673, Korea.
E-mail: yoontae@postech.ac.kr

Copyright © 2020. The Korean Association of Immunologists

This is an Open Access article distributed under the terms of the Creative Commons Attribution Non-Commercial License (<https://creativecommons.org/licenses/by-nc/4.0/>) which permits unrestricted non-commercial use, distribution, and reproduction in any medium, provided the original work is properly cited.

ORCID iDs

Guk-Yeol Park
<https://orcid.org/0000-0002-1075-9040>
Soeun Kim
<https://orcid.org/0000-0002-6425-0899>
Hyebeen Hong
<https://orcid.org/0000-0002-9213-959X>




ABSTRACT

Capicua (CIC) is a transcriptional repressor that regulates several developmental processes. CIC deficiency results in lymphoproliferative autoimmunity accompanied by expansion of CD44^{hi}CD62L^{lo} effector/memory and follicular Th cell populations. Deletion of *Cic* alleles in hematopoietic stem cells (*Vav1-Cre*-mediated knockout of *Cic*) causes more severe autoimmunity than that caused by the knockout of *Cic* in CD4⁺CD8⁺ double positive thymocytes (*Cd4-Cre*-mediated knockout of *Cic*). In this study, we compared splenic CD4⁺ T cell activation and proliferation between whole immune cell-specific *Cic*-null (*Cic^{fl/fl};Vav1-Cre*) and T cell-specific *Cic*-null (*Cic^{fl/fl};Cd4-Cre*) mice. Hyperactivation and hyperproliferation of CD4⁺ T cells were more apparent in *Cic^{fl/fl};Vav1-Cre* mice than in *Cic^{fl/fl};Cd4-Cre* mice. *Cic^{fl/fl};Vav1-Cre* CD4⁺ T cells more rapidly proliferated and secreted larger amounts of IL-2 upon TCR stimulation than did *Cic^{fl/fl};Cd4-Cre* CD4⁺ T cells, while the TCR stimulation-induced activation of the TCR signaling cascade and calcium flux were comparable between them. Mixed wild-type and *Cic^{fl/fl};Vav1-Cre* bone marrow chimeras also exhibited more apparent hyperactivation and hyperproliferation of *Cic*-deficient CD4⁺ T cells than did mixed wild-type and *Cic^{fl/fl};Cd4-Cre* bone marrow chimeras. Taken together, our data demonstrate that CIC deficiency at the beginning of T cell development endows peripheral CD4⁺ T cells with enhanced T cell activation and proliferative capability.

Keywords: Capicua; T-lymphocytes; Lymphocyte activation; Cell proliferation

INTRODUCTION

CD4⁺ Th cells play a pivotal role in the adaptive immune system. CD44^{lo}CD62L^{hi} naïve CD4⁺ T cells are activated by interactions with Ag-presenting cells (APCs) and eventually differentiate into CD44^{hi}CD62L^{lo} effector/memory T cells. Initially, TCR and co-stimulatory receptors on naïve CD4⁺ T cells interact with Ag-presented MHC II molecules and co-stimulatory ligands on APCs, respectively, to provide activation signals to naïve CD4⁺ T cells (1). Activated CD4⁺

Jong Seok Park 
<https://orcid.org/0000-0002-0831-8844>
 Jae-Ho Cho 
<https://orcid.org/0000-0002-3081-7674>
 Yoontae Lee 
<https://orcid.org/0000-0002-6810-3087>

Conflict of Interest

The authors declare no potential conflicts of interest.

Abbreviations

APC, Ag-presenting cell; BM, bone marrow; CIC, Capicua; *Cic^{fl/fl}*; Cd4-Cre, T cell-specific *Cic*-null; *Cic^{fl/fl}*; Vav1-Cre, immune cell-specific *Cic*-null; *Cic^{FLAG/FLAG}*, FLAG-tagged *Cic* knock-in; CTV, cell trace violet; DN, double negative; DP, double positive; GC, germinal center; KO, knockout; MFI, mean fluorescence intensity; PBST, PBS with 0.05% Tween 20; RGEN, RNA-guided endonuclease; sgRNA, single guide RNA; SP, single positive; TBST, Tris buffered saline pH 7.4, 0.1% Tween-20; Tfh, follicular helper T; TMB, 3,3',5,5'-tetramethylbenzidine; WT, wild-type.

Author Contributions

Conceptualization: Park GY, Cho JH, Lee Y; Data curation: Park GY, Lee Y; Formal analysis: Park GY, Lee Y; Funding acquisition: Lee Y; Investigation: Park GY, Lee GW, Kim S, Hong H, Park JS; Project administration: Lee Y; Resources: Lee Y; Supervision: Cho JH, Lee Y; Visualization: Park GY, Lee Y; Writing - original draft: Park GY, Lee Y; Writing - review & editing: Cho JH.

T cells then rapidly proliferate and differentiate into various Th subsets such as Th1, Th2, Th17, and follicular helper T (Tfh) cells according to the cytokines within their surrounding environment (2).

Expansion of the CD44^{hi}CD62L^{lo} effector/memory T cell population is one of the hallmarks of autoimmune diseases (3-6). Hyperactivation and hyperproliferation of CD4⁺ T cells potentially generates a larger population of autoreactive and pathogenic effector Th cells that contribute to the onset of autoimmune diseases. Therefore, alterations in the TCR signaling cascade and downstream target gene expression are associated with the pathogenesis of autoimmune diseases (7-10). Among the Th subsets, Tfh cells mediate the germinal center (GC) response to generate high-affinity Ab-producing plasma cells and memory B cells (11,12). Given the role of Tfh cells in this process, excessive formation and/or hyperactivation of Tfh cells are closely associated with the pathogenesis of Ab-mediated systemic autoimmune diseases such as systemic lupus erythematosus (SLE) (13-15). In support of this, it has been observed that blocking the development or function of Tfh cells alleviates the severity of disease symptoms in lupus mouse models (16,17).

Capicua (CIC) is a high-mobility group box transcription factor that is required for several developmental and physiological processes, including lung and brain development, abdominal wall closure during embryogenesis, and bile acid homeostasis (18-22). CIC also functions as a tumor suppressor in various types of cancer, including prostate, lung, liver, breast, and colorectal cancers, oligodendroglioma, and T cell lymphoma (18,22-30). CIC functions within immune cells have also been studied (6,30,31). Whole immune cell-specific *Cic*-null (*Cic^{fl/fl}*; *Vav1-Cre*) mice develop lymphoproliferative systemic autoimmunity accompanied by increased frequency of CD44^{hi}CD62L^{lo} effector/memory and Tfh cells in the spleen (6). Genetic ablation of *Cic* in T cells by *Cd4-Cre*, which deletes floxed alleles of a specific gene in CD4⁺CD8⁺ double positive (DP) thymocytes (32), also results in systemic autoimmunity (6). However, autoimmune-like phenotypes such as hyperglobulinemia and increased serum autoantibody levels are more severe in *Cic^{fl/fl}*; *Vav1-Cre* mice than in T cell-specific *Cic*-null (*Cic^{fl/fl}*; *Cd4-Cre*) mice (6). This phenomenon could be attributed to 2 possibilities: 1) *Cic*-deficient immune cells other than T cells may contribute to the development of autoimmune-like symptoms in *Cic^{fl/fl}*; *Vav1-Cre* mice, or 2) *Vav1-Cre*-mediated *Cic* deletion in hematopoietic stem cells may produce peripheral T cells with stronger autoimmunity-inducing potential than that caused by the knockout (KO) of *Cic* in DP thymocytes by *Cd4-Cre*.

In this study, we examined the activation and proliferative properties of peripheral CD4⁺ T cells in *Cic^{fl/fl}*; *Vav1-Cre* and *Cic^{fl/fl}*; *Cd4-Cre* mice of the same age. We also compared the effects of *Vav1-Cre*- versus *Cd4-Cre*-mediated T cell-intrinsic loss of *Cic* on T cell activation and proliferation both *in vitro* and *in vivo*.

MATERIALS AND METHODS

Mice

Cic^{fl/fl}; *Cd4-Cre* and *Cic^{fl/fl}*; *Vav1-Cre* mice have been described previously (6). For the experiments, littermates or appropriate age/sex-matched mice were used. FLAG-tagged *Cic* knock-in (*Cic^{FLAG/FLAG}*) mice were created using the CRISPR/Cas9 system, where a single guide RNA (sgRNA) targets the CRISPR/Cas-derived RNA-guided endonuclease (RGEN) site of *Cic* exon 21 to insert 3XFLAG sequences at the 3' end of the *Cic* open reading frame prior to the stop codon.

All mice were maintained in a specific pathogen-free animal facility under a standard 12-h light/12-h dark cycle. Mice were fed standard rodent chow and provided with water *ad libitum*. All experiments were approved by the Institutional Animal Care and Use Committee of Pohang University of Science and Technology.

Flow cytometry analysis

For cell surface staining, cells were stained with fluorochrome-conjugated Abs against cell surface proteins in FACS buffer (PBS with 2% FBS). The following Abs were used: anti-CD4 (RM4-5; BioLegend, San Diego, CA, USA), anti-CD25 (PC61; BioLegend), anti-CD62L (MEL-14; BioLegend), anti-CD69 (H1.2F3; BioLegend), anti-PD-1 (RMP1-30; BioLegend), anti-FLAG (L5; BioLegend), anti-Rat IgG2a κ (RTK2758; BioLegend), anti-CD44 (IM7; BD Bioscience, San Jose, CA, USA), anti-CD62L (MEL-14; BD Bioscience), anti-ICOS (7E.17G9; BD Bioscience), anti-OX-40 (OX-86; eBioscience, San Diego, CA, USA), anti-GITR (DTA-1; eBioscience), anti-Thy1.1 (H1S51; eBioscience), anti-Thy1.2 (53-2.1; eBioscience), anti-CD4 (RM4-5; Tonbo Biosciences, San Diego, CA, USA), and anti-CD44 (IM7; Tonbo Biosciences). For intracellular staining of Ki-67, cells were fixed and permeabilized using Foxp3 Fixation/Permeabilization solution (eBioscience) according to the manufacturer's instructions, and they were then stained with anti-Ki-67 (SO1A15; eBioscience). Dead cells were identified using Ghost Dye (Tonbo Biosciences). The expression of surface and intracellular markers was analyzed using either a CantoII flow cytometer (BD Biosciences) or an LSRII flow cytometer (BD Biosciences).

In vitro T cell proliferation assay

Naïve CD4⁺ T cells were obtained from pooled spleens and lymph nodes of *Cic^{fl/fl}*, *Cic^{fl/fl};Cd4-Cre*, and *Cic^{fl/fl};Vav1-Cre* mice through negative selection (Stemcell Technologies, Vancouver, Canada), and to ensure perfect purity, naïve CD4⁺CD25⁻CD44^{lo} T cells were sorted. The cells were labeled with 5 μ M Cell Trace Violet (CTV; Invitrogen, Carlsbad, CA, USA) for 15 min at 37°C. To remove any free dye remaining in the reaction tubes, 5 times the original staining volume of culture medium (containing 10% FBS) was added, and this was followed by incubation for 5 min. The CTV-labeled cells were activated with plate-bound anti-CD3 (5 μ g/ml) and anti-CD28 (2 μ g/ml) in complete RPMI-1640 medium, incubated at 37°C in a 5% CO₂ incubator, and then collected at 48 h and 72 h after stimulation. The samples were analyzed using a CantoII flow cytometer (BD Biosciences).

ELISA

Sorted naïve CD4⁺ T cells were activated with plate-bound anti-CD3 (5 μ g/ml) and anti-CD28 (2 μ g/ml), and the cell supernatants were collected from cultures at 48 h and 72 h after stimulation. Then, 96-well plates (Corning, New York, NY, USA) were coated with 2 μ g/ml anti-IL-2 (14-7022; eBioscience) at 4°C overnight. The plates were washed with PBS with 0.05% Tween 20 (PBST) and blocked with blocking buffer (PBST containing 2% BSA) at room temperature for 2 h. Standards and diluted samples were added and incubated at room temperature for 2 h. After washing, the plates were incubated with biotin-conjugated anti-IL-2 (13-7021; eBioscience) for 1.5 h followed by incubation with avidin-HRP (18-4100; eBioscience) for 30 min. The plates were developed with 3,3',5,5'-tetramethylbenzidine (TMB) substrate (Surmodics, Eden Prairie, MN, USA) for 30 min and then stopped by adding 1 M H₂SO₄. Absorbance was measured at 450 nm.

Calcium flux measurement

Splenocytes were incubated with 4 μ M Indo-1 (Invitrogen) in RPMI-1640 medium at 37°C for 30 min, and this was followed by washing with RPMI-1640 medium. Indo-1-loaded

splenocytes were incubated with soluble anti-CD3 (0.5 or 1.0 µg/mL) and fluorochrome-conjugated Abs for surface markers (CD4, CD44, and CD62L) in RPMI-1640 medium containing 10% FBS on ice for 20 min and then warmed before cross-linking. A concentration of 25 µg/ml anti-hamster IgG (Jackson ImmunoResearch, West Grove, PA, USA) was added to cross-link anti-CD3 Abs, and the signals were measured by flow cytometry. Ionomycin was added to ensure that T cells were effectively loaded with Indo-1. The emission wavelength ratios of Ca²⁺-bound to unbound Indo-1 were analyzed using an LSRII flow cytometer (BD Biosciences).

Western blot analysis

Sorted naïve CD4⁺ T cells were incubated with soluble anti-CD3 (5 µg/ml) and cross-linked with 25 µg/ml anti-hamster IgG. The cells were incubated at 37°C and collected 2, 10, and 30 min after cross-linking for western blot analysis. Samples were lysed in RIPA buffer (50 mM Tris-HCl pH 7.4, 150 mM NaCl, 1 mM PMSF, 1% NP-40, 0.5% sodium deoxycholate, 0.1% SDS, 1x Roche Complete Protease Inhibitor Cocktail, and 1x Roche Phosphatase Inhibitor Cocktail). Protein concentrations were measured using a BCA kit (Pierce). Equal amounts of protein were prepared and boiled with sample buffer (250 mM Tris-HCl pH 6.8, 50% glycerol, 10% SDS, 5% β-mercaptoethanol, and 0.1% bromophenol blue) for 5 min. The protein samples were separated using 8% SDS-polyacrylamide gel electrophoresis, transferred onto nitrocellulose membranes (Bio-Rad, Hercules, CA, USA), blocked with 5% dry non-fat milk in Tris buffered saline pH 7.4, 0.1% Tween-20 (TBST), washed with TBST, and probed with the following primary Abs in Can get signal solution (Toyobo, Osaka, Japan): anti-CIC (homemade; 1:1,000), anti-p-ZAP70 (SC-12946-R; 1:500), anti-ZAP70 (SC-32760; 1:1,000), anti-p-PLCγ (CST 2821S; 1:500), anti-PLCγ (SC-407; 1:500), anti-p-AKT (CST 9271S; 1:500), anti-AKT (CST 9272; 1:1,000), anti-p-ERK (CST 4370S; 1:500), anti-ERK (CST 9102S; 1:1,000), anti-p-IκBα (CST 2859S; 1:500), anti-IκBα (CST9242S; 1:1,000), and anti-β-actin (SC-32233; 1:2,000). Membranes were incubated with secondary anti-rabbit or anti-mouse IgG Abs conjugated with HRP at room temperature for 1 h, and this was followed by detection using ECL (Bio-Rad) or West DURA (Thermo Scientific, Waltham, MA, USA). Blot images were obtained using ImageQuant LAS 500 (GE Healthcare, Chicago, IL, USA).

Mixed bone marrow (BM) chimera

Bone marrow cells were collected from the tibias and femurs of *Cic^{fl/fl}*, *Cic^{fl/fl};Cd4-Cre*, and *Cic^{fl/fl};Vav1-Cre* mice in RPMI-1640 medium containing 10% FBS and depleted red blood cells with RBC lysis buffer. Equal numbers of BM cells (1×10⁶) from *Cic^{fl/fl}* (Thy1.1/Thy1.2) and *Cic^{fl/fl};Cd4-Cre* (Thy1.1/Thy1.1) mice or *Cic^{fl/fl}* (Thy1.1/Thy1.1) and *Cic^{fl/fl};Vav1-Cre* (Thy1.1/Thy1.2) mice were mixed and transferred to C57BL/6 mice (Thy1.2/Thy1.2) that were lethally irradiated at 10 Gy. Eight weeks later, the mixed BM chimeric mice were sacrificed, and their spleens were analyzed by flow cytometry.

Statistical analysis

Statistical analyses were performed using Prism 8.0 (GraphPad Software, San Diego, CA, USA). One-way ANOVA with Tukey's *post hoc* test was used for multigroup comparisons. Paired 2-tailed Student's *t*-tests were used to compare two groups of mixed BM chimeras. Error bars indicate SEM. A value of *p*<0.05 was considered significant.

RESULTS AND DISCUSSION

Enhanced peripheral CD4⁺ T cell activation in *Cic^{fl/fl};Vav1-Cre* mice

To directly compare the severity of autoimmune-related phenotypes caused by hematopoietic lineage cell-specific versus T cell-specific deletion of *Cic* alleles, we simultaneously analyzed *Cic^{fl/fl}* (WT), *Cic^{fl/fl};Vav1-Cre*, and *Cic^{fl/fl};Cd4-Cre* mice of the same age. Splenomegaly was clearly observed in *Cic^{fl/fl};Vav1-Cre* mice and not in *Cic^{fl/fl};Cd4-Cre* mice irrespective of sex at 12 weeks of age (Fig. 1A). We also analyzed splenic CD4⁺ T cells in these mice. We confirmed our previous findings that the frequency and number of CD44^{hi}CD62L^{lo} effector/memory cells were both significantly increased in *Cic^{fl/fl};Vav1-Cre* mice at the expense of CD44^{lo}CD62L^{hi} naïve CD4⁺ T cells; however, this phenotype was much milder in *Cic^{fl/fl};Cd4-Cre* mice (Fig. 1B). Consistent with these results, the levels of surface molecules representing T cell activation status (CD25^{hi}CD69^{hi}CD44^{hi}CD62L^{lo}) were more dramatically and significantly altered in CD4⁺ T cells from *Cic^{fl/fl};Vav1-Cre* mice (*Vav1-Cre Cic* KO CD4⁺ T cells) compared to those from *Cic^{fl/fl};Cd4-Cre* mice (*Cd4-Cre Cic* KO CD4⁺ T cells) (Fig. 1C). The levels of co-stimulatory molecules, including ICOS, PD-1, OX-40, and GITR, were also higher in *Vav1-Cre Cic* KO CD4⁺ T cells than they were in *Cd4-Cre Cic* KO CD4⁺ T cells (Fig. 1D). Taken together, *Cic^{fl/fl};Vav1-Cre* mice clearly exhibit increased peripheral CD4⁺ T cell hyperactivation compared to that observed in these cells derived from *Cic^{fl/fl};Cd4-Cre* mice.

Increased cell proliferative activity in *Vav1-Cre Cic* KO CD4⁺ T cells

We next examined the cell proliferative activity of *Vav1-Cre* and *Cd4-Cre Cic* KO naïve CD4⁺ T cells by performing an *in vitro* T cell proliferation assay using cell trace violet (CTV) staining. *Vav1-Cre Cic* KO naïve CD4⁺ T cells proliferated faster and secreted higher amounts of IL-2 than did wild-type (WT) cells upon TCR stimulation with an anti-CD3 Ab, and these effects were overridden by co-stimulation with an anti-CD28 Ab (Fig. 2A and B). These findings verified

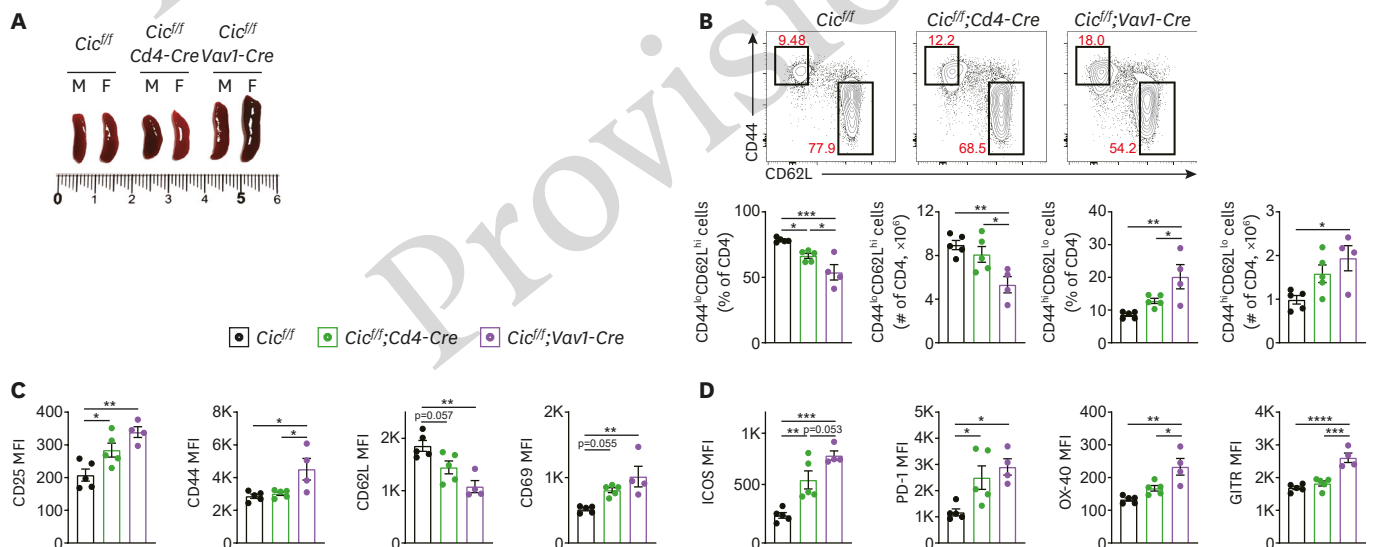


Figure 1. CD4⁺ T cell hyperactivation in *Cic^{fl/fl};Vav1-Cre* mice.

(A) Image of spleens from 12 week-old male (M) and female (F) *Cic^{fl/fl}* (WT), *Cic^{fl/fl};Cd4-Cre*, and *Cic^{fl/fl};Vav1-Cre* mice. (B) FACS analysis showing the proportion of CD44^{lo}CD62L^{hi} naïve CD4⁺ T cells and CD44^{hi}CD62L^{lo} effector/memory CD4⁺ T cells in the spleens of 12 week-old WT, *Cic^{fl/fl};Cd4-Cre*, and *Cic^{fl/fl};Vav1-Cre* mice. Bar graphs show not only the frequency (left) but also the number (right) of naïve and effector/memory CD4⁺ T cells. (C and D) Surface expression levels of activation markers (CD25, CD44, CD62L, and CD69) (C) and co-stimulatory molecules (ICOS, PD-1, OX-40, and GITR) (D) on CD4⁺ T cells in the spleen of WT, *Cic^{fl/fl};Cd4-Cre*, and *Cic^{fl/fl};Vav1-Cre* mice. Bar graphs show data as mean plus or minus the SEM. **p*<0.05, ***p*<0.01, ****p*<0.001, and *****p*<0.0001.

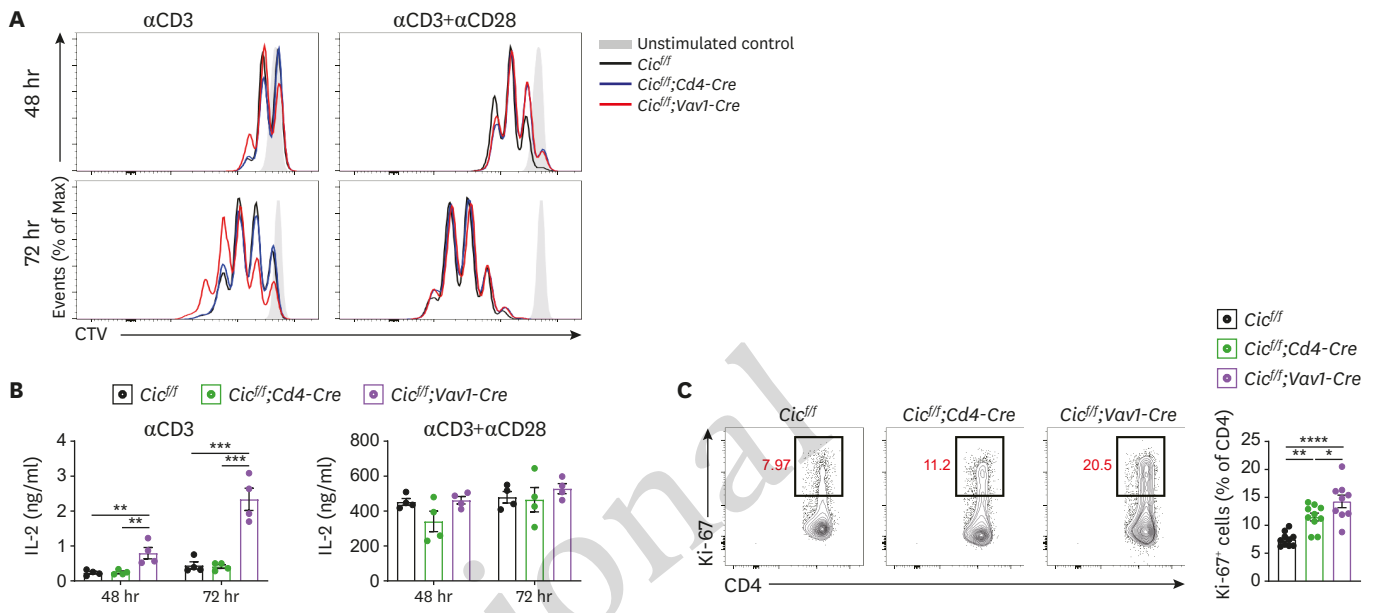


Figure 2. Increased CD4⁺ T cell proliferative capability in *Cic^{fl/fl};Vav1-Cre* mice.

(A) *In vitro* T cell proliferation assay. Naïve CD4⁺ T cells purified from pooled spleens and lymph nodes of WT, *Cic^{fl/fl};Cd4-Cre*, and *Cic^{fl/fl};Vav1-Cre* mice were labelled with CTV dye and stimulated with plate-bound anti-CD3 (5 µg/ml) in the presence (right) or absence (left) of plate-bound anti-CD28 (2 µg/ml). The cells were analyzed at 48 h and 72 h after stimulation. Data are representative of three independent experiments. Shaded area: unstimulated control, black line: *Cic^{fl/fl}*, blue line: *Cic^{fl/fl};Cd4-Cre*, and red line: *Cic^{fl/fl};Vav1-Cre*. (B) ELISA of IL-2. Naïve CD4⁺ T cells purified from pooled spleens and lymph nodes of WT, *Cic^{fl/fl};Cd4-Cre*, and *Cic^{fl/fl};Vav1-Cre* mice were stimulated with plate-bound anti-CD3 (5 µg/ml) in the presence (right) or absence (left) of plate-bound anti-CD28 (2 µg/ml). The supernatants were taken at 48 h and 72 h after stimulation and subjected to ELISA to determine IL-2 concentration. N = 4 per each sample. (C) FACS analysis of Ki-67⁺ CD4⁺ T cells in the spleens of 12 week-old WT, *Cic^{fl/fl};Cd4-Cre*, and *Cic^{fl/fl};Vav1-Cre* mice. n=9 per each genotype of mice. Error bars indicate SEM. *p<0.05, **p<0.01, ***p<0.001, and ****p<0.0001.

our previous results (6). However, the proliferation rate and IL-2 production were comparable between WT and *Cd4-Cre Cic* KO naïve CD4⁺ T cells (Fig. 2A and B), suggesting that the sensitivity to TCR stimulation is different between *Vav1-Cre* and *Cd4-Cre Cic* KO naïve CD4⁺ T cells. We also determined the frequency of *in vivo* proliferating CD4⁺ T cells in the spleens of *Cic^{fl/fl};Vav1-Cre* and *Cic^{fl/fl};Cd4-Cre* mice. The proportion of Ki-67⁺ CD4⁺ T cells was significantly increased in both *Cic^{fl/fl};Cd4-Cre* and *Cic^{fl/fl};Vav1-Cre* mice (Fig. 2C). Notably, *Cic^{fl/fl};Vav1-Cre* mice exhibited a higher frequency of Ki-67⁺ CD4⁺ T cells than did *Cic^{fl/fl};Cd4-Cre* mice (Fig. 2C). These results indicate that *Vav1-Cre Cic* KO CD4⁺ T cells possessed enhanced cell proliferative capability compared to that of *Cd4-Cre Cic* KO CD4⁺ T cells.

Comparable calcium flux and activation of TCR signaling cascades in CD4⁺ T cells from WT, *Cic^{fl/fl};Cd4-Cre*, and *Cic^{fl/fl};Vav1-Cre* mice

As TCR stimulation-induced cell proliferation and IL-2 secretion were significantly increased in *Vav1-Cre Cic* KO naïve CD4⁺ T cells compared to these processes in WT or *Cd4-Cre Cic* KO CD4⁺ naïve T cells (Fig. 2A and B), we examined the activation of the TCR signaling pathway in the same set of cells when treated with an anti-CD3 Ab. Unexpectedly, neither calcium flux nor the levels of phosphorylated TCR signaling components, including ZAP70, PLCγ, AKT, ERK, and IκBα, were increased in *Vav1-Cre Cic* KO CD4⁺ T cells (Fig. 3A and B). The levels of phosphorylated ERK were slightly decreased in both *Cd4-Cre* and *Vav1-Cre Cic* KO CD4⁺ T cells (Fig. 3B). This result may be due to derepression of CIC target genes such as *Spry4*, *Spred1*, and *Dusp4* that are involved in the dephosphorylation of ERK, as levels of these genes have been reported to be upregulated in *Cic*-deficient naïve CD4⁺ T cells (6). These findings suggest that CIC deficiency-induced CD4⁺ T cell activation and proliferation may occur independently of activation of TCR signaling cascade components and calcium flux.

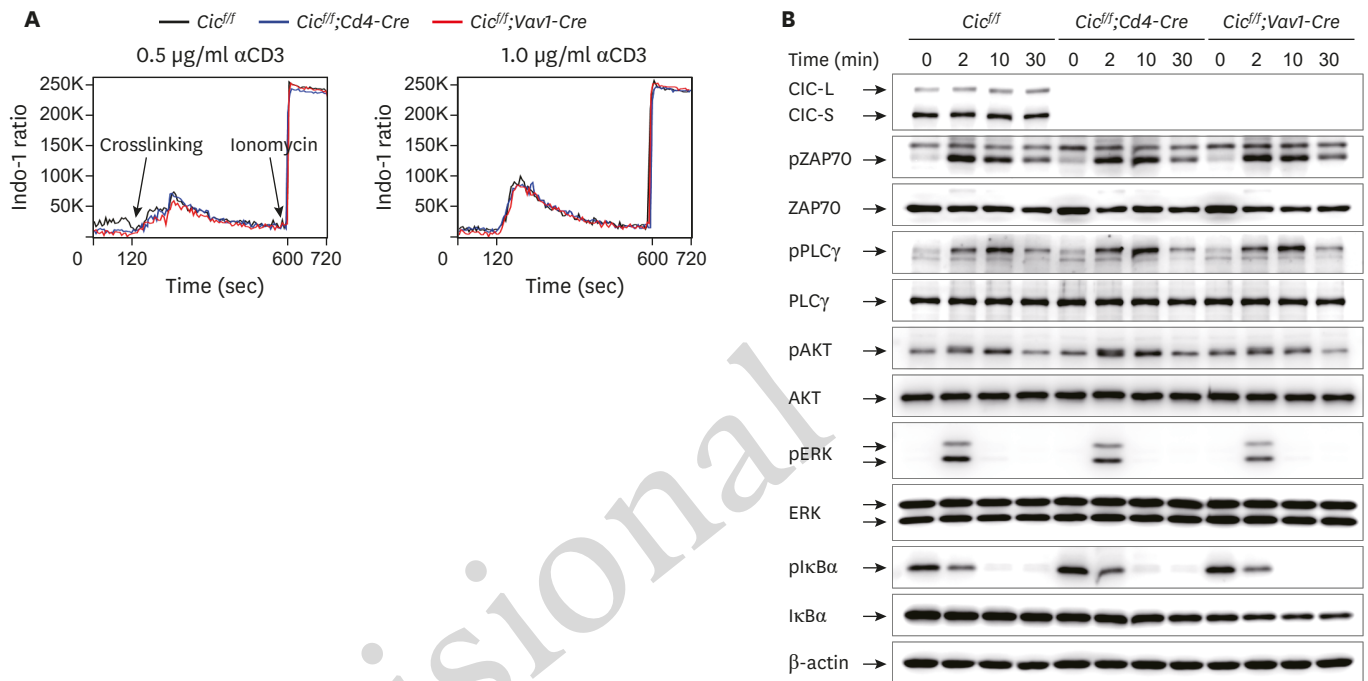


Figure 3. Comparison of the activation of the TCR signaling cascade and calcium flux in CD4⁺ T cells from WT, *Cic^{fl/fl};Cd4-Cre*, and *Cic^{fl/fl};Vav1-Cre* mice upon TCR stimulation. (A) Representative calcium flux profiles of WT, *Cic^{fl/fl};Cd4-Cre*, and *Cic^{fl/fl};Vav1-Cre* naïve CD4⁺ T cells. For stimulation, anti-hamster IgG cross-linker was added at 120 s, and ionomycin was used to measure saturated Ca²⁺ levels as positive control. Data are representative of three independent experiments. Black line: *Cic^{fl/fl}*, blue line: *Cic^{fl/fl};Cd4-Cre*, and red line: *Cic^{fl/fl};Vav1-Cre*. (B) Western blot analysis to assess the levels of activated TCR signaling cascade components. Naïve CD4⁺ T cells purified from pooled spleens and lymph nodes of WT, *Cic^{fl/fl};Cd4-Cre*, and *Cic^{fl/fl};Vav1-Cre* mice were stimulated with anti-CD3 and subjected to western blot analysis. At least three independent experiments were conducted.

T cell-intrinsic effect of *CIC* loss on the hyperactivation and hyperproliferation of peripheral CD4⁺ T cells in *Cic^{fl/fl};Vav1-Cre* mice

We showed that hyperactivation and hyperproliferation of CD4⁺ T cells were more apparent in *Cic^{fl/fl};Vav1-Cre* than in *Cic^{fl/fl};Cd4-Cre* mice (Figs. 1B and 2C). Because *Vav1-Cre* deletes floxed alleles of a specific gene not only in T cells but also in other types of immune cells (33), it is unclear if the enhanced hyperactivation and hyperproliferation of splenic CD4⁺ T cells in *Cic^{fl/fl};Vav1-Cre* mice were T cell-intrinsic or -extrinsic. To clarify this issue, we generated mixed BM chimeric mice by transferring the same number of BM cells from Thy1.1/Thy1.2 heterozygous WT and Thy1.1/Thy1.1 homozygous *Cic^{fl/fl};Cd4-Cre* mice (WT:*Cic^{fl/fl};Cd4-Cre* BM chimera) or Thy1.1/Thy1.1 homozygous WT and Thy1.1/Thy1.2 heterozygous *Cic^{fl/fl};Vav1-Cre* mice (WT:*Cic^{fl/fl};Vav1-Cre* BM chimera) into irradiated Thy1.2/Thy1.2 homozygous WT recipient mice (Fig. 4A), and analyzed splenic CD4⁺ T cells in these chimeric mice. Consistent with the results from the analyses of CD4⁺ T cells in WT, *Cic^{fl/fl};Cd4-Cre*, and *Cic^{fl/fl};Vav1-Cre* mice (Fig. 1B), not only *Cic^{fl/fl};Vav1-Cre* but also *Cic^{fl/fl};Cd4-Cre* BM cells preferentially gave rise to CD44^{hi}CD62L^{lo} effector/memory CD4⁺ T cells at the expense of CD44^{lo}CD62L^{hi} naïve CD4⁺ T cells when compared to those from WT mice (Fig. 4B and C). Importantly, the fold changes in the frequency of CD44^{lo}CD62L^{hi} naïve and CD44^{hi}CD62L^{lo} effector/memory CD4⁺ T cells between WT and *Cic*-deficient CD4⁺ T cell compartments were more dramatic in the WT:*Cic^{fl/fl};Vav1-Cre* BM chimeras than they were in the WT:*Cic^{fl/fl};Cd4-Cre* BM chimeras (Fig. 4C). Consistent with this result, the surface expression levels of CD44 and CD62L were more dramatically increased and decreased, respectively, on the *Vav1-Cre Cic* KO CD4⁺ T cells compared to those on the *Cd4-Cre Cic* KO CD4⁺ T cells (Fig. 4D and E). These data demonstrate that the enhanced CD4⁺ T cell hyperactivation in *Cic^{fl/fl};Vav1-Cre* mice in comparison with that in *Cic^{fl/fl};Cd4-Cre* mice is at

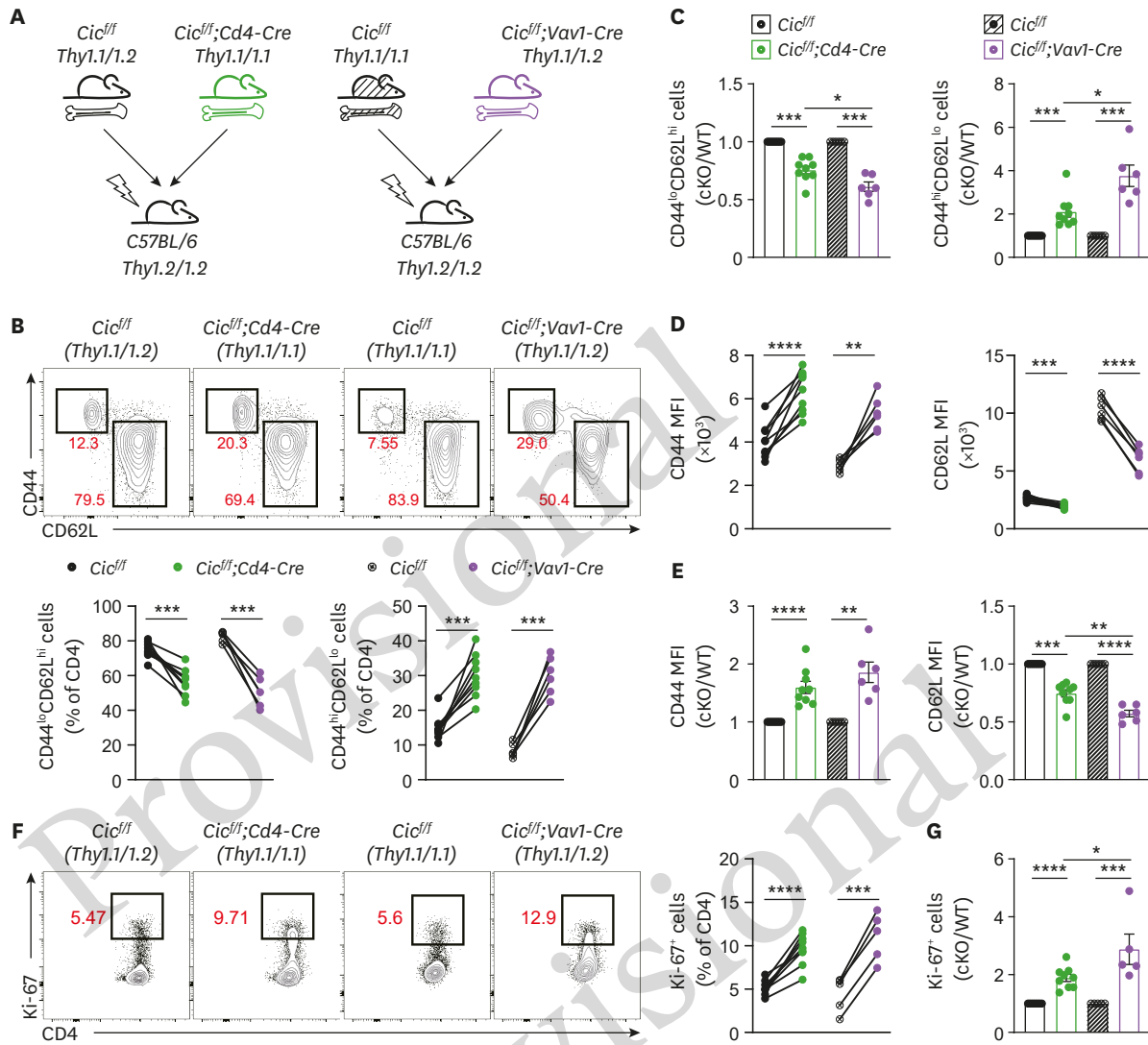


Figure 4. *Vav1-Cre*-mediated T cell-intrinsic loss of CIC leads to hyperactivation and hyperproliferation of CD4⁺ T cells. (A) Schematic illustration for the generation of chimeric mice with WT, *Cic^{fl/fl};Cd4-Cre*, and *Cic^{fl/fl};Vav1-Cre* BM cells. (B) FACS analysis for the proportion of splenic CD44^{lo}CD62L^{hi} naive and CD44^{hi}CD62L^{lo} effector/memory cells in the CD4⁺ T cell compartments of either WT (Thy1.1/Thy1.2) and *Cic^{fl/fl};Cd4-Cre* (Thy1.1/Thy1.1) or WT (Thy1.1/Thy1.1) and *Cic^{fl/fl};Vav1-Cre* (Thy1.1/Thy1.2) mixed BM chimeric mice. (C) Relative fold changes in the frequency of CD44^{lo}CD62L^{hi} naive and CD44^{hi}CD62L^{lo} effector/memory cells between WT and *Cic*-deficient (cKO) CD4⁺ T cell compartments of the mixed BM chimeric mice. The relative fold changes were calculated based on the results in (B). (D) Surface expression levels of CD44 and CD62L on splenic CD4⁺ T cells from the mixed BM chimeric mice. Graphs show a pairwise comparison between WT and *Cic*-deficient (cKO) CD4⁺ T cells in the same mixed BM chimeric mice. (E) Relative fold changes in the levels of CD44 and CD62L on splenic CD4⁺ T cells between WT and *Cic*-deficient (cKO) CD4⁺ T cell compartments of the mixed BM chimeric mice. The relative fold changes were calculated based on the results in (D). (F) FACS analysis for the frequency of splenic Ki-67⁺ cells in the CD4⁺ T cell compartments of either WT (Thy1.1/Thy1.2) and *Cic^{fl/fl};Cd4-Cre* (Thy1.1/Thy1.1) or WT (Thy1.1/Thy1.1) and *Cic^{fl/fl};Vav1-Cre* (Thy1.1/Thy1.2) mixed BM chimeric mice. Graphs show a pairwise comparison between WT and *Cic*-deficient (cKO) CD4⁺ T cells in the same mixed BM chimeric mice. (G) Relative fold changes in the frequency of Ki-67⁺ cells between WT and *Cic*-deficient (cKO) CD4⁺ T cell compartments of the mixed BM chimeric mice. The relative fold changes were calculated based on the results in (F). WT (Thy1.1/Thy1.2) and *Cic^{fl/fl};Cd4-Cre* (Thy1.1/Thy1.1) mixed BM chimeric mice (n=9) and WT (Thy1.1/Thy1.1) and *Cic^{fl/fl};Vav1-Cre* (Thy1.1/Thy1.2) mixed BM chimeric mice (n=5-6). *p<0.05, **p<0.01, ***p<0.001, and ****p<0.0001.

least in part due to T cell-intrinsic loss of CIC. The *Cic*-deficient CD4⁺ T cells also expressed higher levels of co-stimulatory molecules, including ICOS, PD-1, and OX-40, than did the WT counterparts in WT: *Cic^{fl/fl};Cd4-Cre* as well as WT: *Cic^{fl/fl};Vav1-Cre* BM chimeras (**Supplementary Fig. 1**). However, the fold increases in the levels of co-stimulatory molecules on *Cic*-deficient versus WT CD4⁺ T cells were comparable between WT: *Cic^{fl/fl};Vav1-Cre* and WT: *Cic^{fl/fl};Cd4-Cre* BM

chimeras (**Supplementary Fig. 1**), suggesting that the increased expression levels of co-stimulatory molecules on CD4⁺ T cells in *Cic^{fl/fl};Vav1-Cre* mice (**Fig. 1D**) might be attributed to both T cell-intrinsic and -extrinsic loss of CIC. We also examined CD4⁺ T cell proliferation in these mice by conducting Ki-67 staining. Consistent with the previous data (**Fig. 2C**), the frequency of Ki-67⁺ cells was significantly increased in the compartments of *Vav1-Cre* and *Cd4-Cre Cic* KO CD4⁺ T cells compared to that in WT CD4⁺ T cell compartments (**Fig. 4F and G**). Moreover, the fold increase in the frequency of Ki-67⁺ cells between WT and *Cic*-deficient CD4⁺ T cell compartments was greater in the WT:*Cic^{fl/fl};Vav1-Cre* BM chimeras than in the WT:*Cic^{fl/fl};Cd4-Cre* BM chimeras (**Fig. 4G**). Taken together, these results demonstrate that both hyperactivation and hyperproliferation of peripheral CD4⁺ T cells in *Cic^{fl/fl};Vav1-Cre* mice were due to T cell-intrinsic loss of CIC rather than CIC deficiency in other types of immune cells.

Our study revealed that *Vav1-Cre*-mediated removal of *Cic* alleles endows peripheral CD4⁺ T cells with stronger activation potential and proliferative capability than that mediated by *Cd4-Cre*, and that the hyperactivation and hyperproliferation of *Vav1-Cre Cic* KO CD4⁺ T cells are T cell-intrinsic phenotypes. In line with this idea, we observed that the frequency of CD44^{lo}CD62L^{hi} naïve and CD44^{hi}CD62L^{lo} effector/memory CD4⁺ T cells was normal in the spleens of B cell-specific (*Cic^{fl/fl};Cd19-Cre*) and dendritic cell-specific (*Cic^{fl/fl};Cd11c-Cre*) *Cic* null mice (unpublished data). These findings raise the interesting possibility that CIC deficiency prior to the DP stage of thymic T cell development could affect mature CD4⁺ T cell activation and proliferation properties, as *Vav1* is expressed in hematopoietic stem cells and *Cd4* is expressed in DP thymocytes (32,33). Tan *et al.* (30) have shown that CIC deficiency increases the frequency of CD4⁻CD8⁻ double negative 1 (DN1) thymocytes, suggesting a potential role of CIC in the regulation of thymic T cell development. Consistent with this notion, we found that CIC levels were higher in DN thymocytes than they were in DP and single positive (SP) thymic T cells (**Supplementary Fig. 2**). A more detailed study examining the role of CIC in thymic T cell development will improve our understanding of how CIC suppresses peripheral T cell activation and proliferation to ultimately regulate autoimmunity.

ACKNOWLEDGEMENTS

We thank the Lee lab members for helpful discussions and comments on this study. This work was supported by grants from the Samsung Science and Technology Foundation under project number SSTF-BA1502-14 and the National Research Foundation (NRF) of Korea (2017R1A5A1015366 and 2018R1A2B2004416 for YL; 2018R1A5A2024181 and 2020M3A9G3080281 for JHC). GYP, HH, SK, and JSP were supported by the BK21 Program.

SUPPLEMENTARY MATERIALS

Supplementary Figure 1

Surface expression levels of ICOS, PD-1, and OX-40 on splenic CD4⁺ T cells from mixed BM chimeric mice.

[Click here to view](#)

Supplementary Figure 2

CIC protein levels in CD4⁻CD8⁻ DN, CD4⁺CD8⁺ DP, CD4⁺ SP (4SP), and CD8⁺ SP (8SP) thymocytes.

[Click here to view](#)

REFERENCES

1. Sharma P, Wagner K, Wolchok JD, Allison JP. Novel cancer immunotherapy agents with survival benefit: recent successes and next steps. *Nat Rev Cancer* 2011;11:805-812.
[PUBMED](#) | [CROSSREF](#)
2. Srivastava RK, Dar HY, Mishra PK. Immunoporosis: immunology of osteoporosis-role of t cells. *Front Immunol* 2018;9:657.
[PUBMED](#) | [CROSSREF](#)
3. Devarajan P, Chen Z. Autoimmune effector memory T cells: the bad and the good. *Immunol Res* 2013;57:12-22.
[PUBMED](#) | [CROSSREF](#)
4. Kim CJ, Lee CG, Jung JY, Ghosh A, Hasan SN, Hwang SM, Kang H, Lee C, Kim GC, Rudra D, et al. The transcription factor Ets1 suppresses T follicular helper type 2 cell differentiation to halt the onset of systemic lupus erythematosus. *Immunity* 2019;50:272.
[PUBMED](#) | [CROSSREF](#)
5. Vinuesa CG, Cook MC, Angelucci C, Athanasopoulos V, Rui L, Hill KM, Yu D, Domaschensch H, Whittle B, Lambie T, et al. A RING-type ubiquitin ligase family member required to repress follicular helper T cells and autoimmunity. *Nature* 2005;435:452-458.
[PUBMED](#) | [CROSSREF](#)
6. Park S, Lee S, Lee CG, Park GY, Hong H, Lee JS, Kim YM, Lee SB, Hwang D, Choi YS, et al. Capicua deficiency induces autoimmunity and promotes follicular helper T cell differentiation via derepression of ETV5. *Nat Commun* 2017;8:16037.
[PUBMED](#) | [CROSSREF](#)
7. Krishnan S, Juang YT, Chowdhury B, Magilavy A, Fisher CU, Nguyen H, Nambiar MP, Kyttaris V, Weinstein A, Bahjat R, et al. Differential expression and molecular associations of Syk in systemic lupus erythematosus T cells. *J Immunol* 2008;181:8145-8152.
[PUBMED](#) | [CROSSREF](#)
8. Chan AY, Punwani D, Kadlecck TA, Cowan MJ, Olson JL, Mathes EF, Sunderam U, Fu SM, Srinivasan R, Kuriyan J, et al. A novel human autoimmune syndrome caused by combined hypomorphic and activating mutations in ZAP-70. *J Exp Med* 2016;213:155-165.
[PUBMED](#) | [CROSSREF](#)
9. Suzuki A, Yamaguchi MT, Ohteki T, Sasaki T, Kaisho T, Kimura Y, Yoshida R, Wakeham A, Higuchi T, Fukumoto M, et al. T cell-specific loss of Pten leads to defects in central and peripheral tolerance. *Immunity* 2001;14:523-534.
[PUBMED](#) | [CROSSREF](#)
10. Chang M, Jin W, Chang JH, Xiao Y, Brittain GC, Yu J, Zhou X, Wang YH, Cheng X, Li P, et al. The ubiquitin ligase Peli1 negatively regulates T cell activation and prevents autoimmunity. *Nat Immunol* 2011;12:1002-1009.
[PUBMED](#) | [CROSSREF](#)
11. Crotty S. Follicular helper CD4 T cells (TFH). *Annu Rev Immunol* 2011;29:621-663.
[PUBMED](#) | [CROSSREF](#)
12. Nurieva RI, Chung Y. Understanding the development and function of T follicular helper cells. *Cell Mol Immunol* 2010;7:190-197.
[PUBMED](#) | [CROSSREF](#)
13. Craft JE. Follicular helper T cells in immunity and systemic autoimmunity. *Nat Rev Rheumatol* 2012;8:337-347.
[PUBMED](#) | [CROSSREF](#)
14. Crotty S. T follicular helper cell biology: a decade of discovery and diseases. *Immunity* 2019;50:1132-1148.
[PUBMED](#) | [CROSSREF](#)
15. Ryu H, Kim J, Kim D, Lee JE, Chung Y. Cellular and molecular links between autoimmunity and lipid metabolism. *Mol Cells* 2019;42:747-754.
[PUBMED](#) | [CROSSREF](#)

16. Yang J, Yang X, Yang J, Li M. Baicalin ameliorates lupus autoimmunity by inhibiting differentiation of Tfh cells and inducing expansion of Tfr cells. *Cell Death Dis* 2019;10:140.
[PUBMED](#) | [CROSSREF](#)
17. Lee SK, Silva DG, Martin JL, Pratama A, Hu X, Chang PP, Walters G, Vinuesa CG. Interferon- γ excess leads to pathogenic accumulation of follicular helper T cells and germinal centers. *Immunity* 2012;37:880-892.
[PUBMED](#) | [CROSSREF](#)
18. Lee Y. Regulation and function of Capicua in mammals. *Exp Mol Med* 2020;52:531-537.
[PUBMED](#) | [CROSSREF](#)
19. Kim E, Park S, Choi N, Lee J, Yoe J, Kim S, Jung HY, Kim KT, Kang H, Fryer JD, et al. Deficiency of Capicua disrupts bile acid homeostasis. *Sci Rep* 2015;5:8272.
[PUBMED](#) | [CROSSREF](#)
20. Lee Y, Fryer JD, Kang H, Crespo-Barreto J, Bowman AB, Gao Y, Kahle JJ, Hong JS, Kheradmand F, Orr HT, et al. ATXN1 protein family and CIC regulate extracellular matrix remodeling and lung alveolarization. *Dev Cell* 2011;21:746-757.
[PUBMED](#) | [CROSSREF](#)
21. Lu HC, Tan Q, Rousseaux MW, Wang W, Kim JY, Richman R, Wan YW, Yeh SY, Patel JM, Liu X, et al. Disruption of the ATXN1-CIC complex causes a spectrum of neurobehavioral phenotypes in mice and humans. *Nat Genet* 2017;49:527-536.
[PUBMED](#) | [CROSSREF](#)
22. Simón-Carrasco L, Graña O, Salmón M, Jacob HK, Gutierrez A, Jiménez G, Drosten M, Barbacid M. Inactivation of Capicua in adult mice causes T-cell lymphoblastic lymphoma. *Genes Dev* 2017;31:1456-1468.
[PUBMED](#) | [CROSSREF](#)
23. Bunda S, Heir P, Metcalf J, Li AS, Agnihotri S, Pusch S, Yasin M, Li M, Burrell K, Mansouri S, et al. CIC protein instability contributes to tumorigenesis in glioblastoma. *Nat Commun* 2019;10:661.
[PUBMED](#) | [CROSSREF](#)
24. Kim E, Kim D, Lee JS, Yoe J, Park J, Kim CJ, Jeong D, Kim S, Lee Y. Capicua suppresses hepatocellular carcinoma progression by controlling the ETV4-MMP1 axis. *Hepatology* 2018;67:2287-2301.
[PUBMED](#) | [CROSSREF](#)
25. Lee JS, Kim E, Lee J, Kim D, Kim H, Kim CJ, Kim S, Jeong D, Lee Y. Capicua suppresses colorectal cancer progression via repression of ETV4 expression. *Cancer Cell Int* 2020;20:42.
[PUBMED](#) | [CROSSREF](#)
26. Okimoto RA, Breitenbuecher F, Olivas VR, Wu W, Gini B, Hofree M, Asthana S, Hrustanovic G, Flanagan J, Tulpule A, et al. Inactivation of Capicua drives cancer metastasis. *Nat Genet* 2017;49:87-96.
[PUBMED](#) | [CROSSREF](#)
27. Yoe J, Kim D, Kim S, Lee Y. Capicua restricts cancer stem cell-like properties in breast cancer cells. *Oncogene* 2020;39:3489-3506.
[PUBMED](#) | [CROSSREF](#)
28. Bettgowda C, Agrawal N, Jiao Y, Sausen M, Wood LD, Hruban RH, Rodriguez FJ, Cahill DP, McLendon R, Riggins G, et al. Mutations in *CIC* and *FUBP1* contribute to human oligodendroglioma. *Science* 2011;333:1453-1455.
[PUBMED](#) | [CROSSREF](#)
29. Gleize V, Alentorn A, Connen de Kérillis L, Labussière M, Nadaradjane AA, Mundwiller E, Ottolenghi C, Mangesius S, Rahimian A, Ducray F, et al. *CIC* inactivating mutations identify aggressive subset of 1p19q codeleted gliomas. *Ann Neurol* 2015;78:355-374.
[PUBMED](#) | [CROSSREF](#)
30. Tan Q, Brunetti L, Rousseaux MW, Lu HC, Wan YW, Revelli JP, Liu Z, Goodell MA, Zoghbi HY. Loss of Capicua alters early T cell development and predisposes mice to T cell lymphoblastic leukemia/lymphoma. *Proc Natl Acad Sci U S A* 2018;115:E1511-E1519.
[PUBMED](#) | [CROSSREF](#)
31. Park S, Park J, Kim E, Lee Y. The Capicua/ETS translocation variant 5 axis regulates liver-resident memory CD8⁺ T-cell development and the pathogenesis of liver injury. *Hepatology* 2019;70:358-371.
[PUBMED](#) | [CROSSREF](#)
32. Lee PP, Fitzpatrick DR, Beard C, Jessup HK, Lehar S, Makar KW, Pérez-Melgosa M, Sweetser MT, Schlissel MS, Nguyen S, et al. A critical role for Dnmt1 and DNA methylation in T cell development, function, and survival. *Immunity* 2001;15:763-774.
[PUBMED](#) | [CROSSREF](#)
33. de Boer J, Williams A, Skavdis G, Harker N, Coles M, Tolaini M, Norton T, Williams K, Roderick K, Potocnik AJ, et al. Transgenic mice with hematopoietic and lymphoid specific expression of Cre. *Eur J Immunol* 2003;33:314-325.
[PUBMED](#) | [CROSSREF](#)